



## Manganese removal from groundwater: characterization of filter media coating

Jantinus H. Bruins<sup>a,b,c,\*</sup>, Branislav Petrusevski<sup>b</sup>, Yness M. Slokar<sup>b</sup>, Joop C. Kruithof<sup>b,d</sup>, Maria D. Kennedy<sup>b,c</sup>

<sup>a</sup>WLN, Rijksweg 85, 9756 AD, Glimmen, The Netherlands, Tel. +31 (0)50 4022121; Fax: +31 (0)50 4094274; email: [j.bruins@wln.nl](mailto:j.bruins@wln.nl) (J.H. Bruins)

<sup>b</sup>UNESCO-IHE Institute for Water Education, Westvest 7, 2611 AX, Delft, The Netherlands, Tel. +31 (0)15 2151785; email: [b.petrusevski@unesco-ihe.org](mailto:b.petrusevski@unesco-ihe.org) (B. Petrusevski), Tel. +31 (0)6 2151826; email: [y.slokar@unesco-ihe.org](mailto:y.slokar@unesco-ihe.org) (Y.M. Slokar), Tel. +31 (0)6 53165153; email: [joop.kruithof@planet.nl](mailto:joop.kruithof@planet.nl) (J.C. Kruithof), Tel. +31 (0)15 2151774; Fax: +31 (0)15 21222921; email: [m.kennedy@unesco-ihe.org](mailto:m.kennedy@unesco-ihe.org) (M.D. Kennedy)

<sup>c</sup>Technical University Delft, Stevinweg 1, 2628 CN, Delft, The Netherlands

<sup>d</sup>Wetsus, Centre of Excellence for Sustainable Water Technology, P.O. Box 1113, 8900 CC, Leeuwarden, The Netherlands

Received 6 February 2014; Accepted 20 May 2014

---

### ABSTRACT

Removal of manganese in conventional aeration-filtration groundwater treatment plants (GWTPs) results in the formation of a manganese oxide coating on filter media. The formation of this coating is an essential prerequisite for efficient manganese removal. Different manganese oxides have varying affinities for autocatalytic adsorption/oxidation of dissolved manganese. The aim of this study was to characterize manganese oxide(s) on filter media from successfully operating manganese removal plants. Characterization of filter media samples from full-scale groundwater treatment plants and identification of manganese species was carried out by X-ray diffraction, scanning electron microscopy coupled with energy dispersive X-radiation (SEM-EDX), Raman spectroscopy and electron paramagnetic resonance (EPR). The results showed that the manganese oxide present in the aged coating was poorly crystalline. Results from the Raman spectroscopy and the detailed EPR analysis show that the manganese oxide in the ripened coating was of a Birnessite type, and of physicochemical origin. The results transpiring from this research suggest that the presence of Birnessite in the coating is essential for effective manganese removal in conventional aeration-filtration treatment plants, since Birnessite has a considerable ability to adsorb and oxidize dissolved manganese.

*Keywords:* Groundwater treatment; Manganese removal; MOCS; Filter media characterization; Birnessite

---

---

\*Corresponding author.

## 1. Introduction

### 1.1. General

Groundwater is the most abundant source for drinking water production, representing over 90% of the world's readily available freshwater. About 1.5 billion people depend upon groundwater for their drinking water supply [1]. In addition to iron and ammonium, groundwater frequently contains elevated concentrations of dissolved manganese, which should be lowered for both health and aesthetic reasons. In European countries, the removal of manganese from groundwater is commonly achieved by aeration-rapid sand filtration, eliminating the need for oxidant to enhance manganese oxidation. This type of manganese removal is effective and beneficial for both environmental and economic reasons, but requires a long ripening period of virgin filter media. The ripening time can last from several weeks to more than a year, before effective manganese removal is achieved [2–4].

Although extensive research has been carried out on manganese removal by aeration-rapid sand filtration, the mechanisms controlling the ripening period, including the formation of a manganese oxide coating on virgin filter media, are still not well understood. Several researchers have suggested that the use of (pre)coated or (“bio”) aged filter media can shorten the ripening period [5–15]. Aged filter media in manganese removal filters typically consists of manganese oxide-coated sand (MOCS) and/or manganese oxide-coated anthracite (MOCA). Autocatalytic properties that are attributed to the coating of these filter media enhance the adsorption of dissolved manganese and its subsequent oxidation. The ripening time of filter media is controlled by the type and amount of manganese oxide(s) present in the coating. As proposed by Stumm and Morgan [16], oxidation of manganese in homogeneous aqueous solution follows different pathways, as shown in a simplified scheme (Fig. 1).

The propensity of manganese present in filter media coating heavily depends on the valence of manganese in the oxide [17]. A higher valence restricts the

possibility of further oxidation. The valences of manganese oxides shown in Fig. 1 are given in Table 1.

In nature, the most stable form of manganese oxide is Pyrolusite ( $\beta\text{MnO}_2$ ). Because the valence of manganese in this oxide is 4, no further oxidation can take place. Pyrolusite has a large adsorption capacity, but no autocatalytic oxidative properties [6]. Consequently, when the adsorption capacity is exhausted, the removal of manganese stops.

Pyrolusite is formed when (powerful) oxidants such as chlorine ( $\text{Cl}_2$ ), chlorine dioxide ( $\text{ClO}_2$ ), ozone ( $\text{O}_3$ ) or potassium permanganate ( $\text{KMnO}_4$ ) are used. These oxidants are commonly applied in countries such as the USA [19,20]. Pre-oxidation with powerful oxidants can achieve a very effective manganese removal. However, this type of process is associated with disadvantages such as continuous oxidant dosage to achieve manganese removal. This process is also associated with high costs and environmental risks, and requires accurate oxidant dosage: under dosing causes incomplete manganese oxidation, and consequently a poor manganese removal, while overdosing with permanganate gives the water a pinkish colour. Therefore in Western European countries, such as The Netherlands, manganese removal by conventional groundwater treatment with aeration-filtration is preferred.

Based on thermodynamic considerations, the following pathway for manganese oxidation in water is proposed: (Pyrochroite)—Hausmannite—Manganite—Pyrolusite [21,22]. However, based on the  $p\varepsilon/\text{pH}$  diagram shown in Fig. 2 [16], chemical formation of Pyrochroite ( $\text{Mn}(\text{OH})_2$ ) under common groundwater conditions (pH 6–8) is unlikely. Without a catalyst, the pH must be at least 8.6 to achieve Hausmannite ( $\text{Mn}_3\text{O}_4$  formation), which is subsequently removed by filtration [21]. Formation of Pyrochroite requires an even higher pH, of at least 11.

The exact pathway by which manganese oxidation occurs under conditions commonly applied in groundwater treatment, is not known. Besides chemical oxidation, “biology” may play an important role.

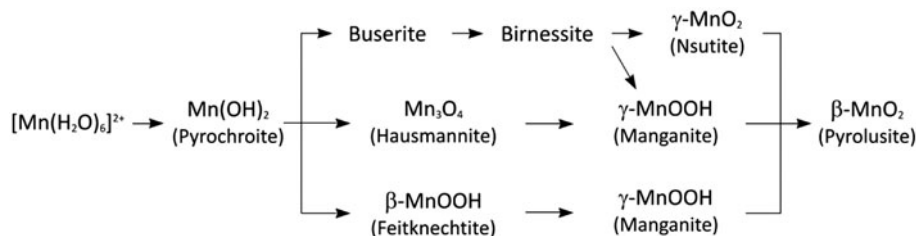


Fig. 1. Simplified scheme of  $\text{Mn}^{2+}$  oxidation pathways according to Stumm and Morgan [16].

Table 1  
Types of manganese oxide and the average valence of manganese in these oxides

Manganese oxide	Valence of manganese
Pyrochroite	2 [16]
Hausmannite	~2.7 [17]
Manganite/Feitknechtite	3 [17]
Buserite/Birnessite	3.5–3.9 [18]
Nsutite	~4 [17]
Pyrolusite	4 [17]

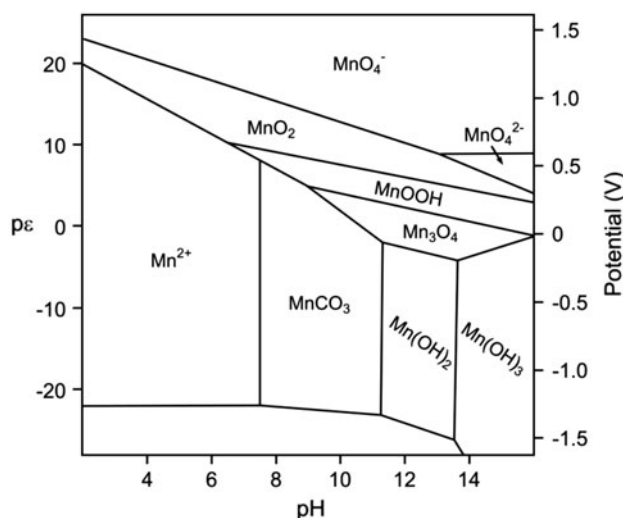


Fig. 2. Diagram of electron activity ( $p_e$ ) and redox potential ( $E_h$  in V) as a function of the pH showing the stability zones of manganese-containing compounds in aqueous solution.

Source: adopted from Stumm and Morgan [16].

Identification of the manganese oxide(s) present in filter media coatings from manganese removal filters might give insight into the formation of manganese oxide coatings on virgin filter media. This may elucidate the mechanisms controlling the start-up of the manganese removal process [23]. Based on these results, recommendations for process modifications to shorten the ripening period of manganese removal filters may be made.

### 1.2. Aim of this study

The aim of this study was to characterize the coating of MOCS and MOCA from (ripened) manganese removal filters in full-scale groundwater treatment plants (GWTPs), by identification of the types of manganese oxide present in the coating. It was hypothesized that identification of the manganese oxide

present in ripened media from manganese removal filters may help to better understand the driving force behind efficient manganese removal in conventional aeration-filtration groundwater treatment plants.

## 2. Materials and methods

MOCS and MOCA characterized in this study were collected from two GWTPs of two water companies as follows.

- MOCS from GWTP De Punt (Groningen, The Netherlands).

The sample was taken from a depth of 140–150 cm, from a filter bed that was removed after an operating time of approximately 15 years.

- MOCA from GWTP Grobbendonk (Pidpa, Belgium).

The sample was taken from the top of a filter bed, in operation for more than 12 years.

Both GWTPs utilize conventional groundwater treatment by aeration-filtration and achieve complete manganese removal. Information on feed water quality, process design parameters and operational conditions of full-scale plants De Punt and Grobbendonk are shown in Table 2.

To characterize the filter media coatings and to identify the manganese oxide(s), the following supplementary techniques were used:

- Raman spectroscopy;
- X-ray diffraction (XRD);
- Scanning electron microscopy coupled with energy dispersive X-radiation analysis (SEM-EDX); and
- Electron paramagnetic resonance (EPR).

As these techniques are supplementary, for complete identification and determination of the origin of produced  $MnO_x$ , application of all these methods is required. Use of one single method is insufficient to characterize and identify the manganese oxides.

For additional information with respect to Raman spectroscopy (selection spectroscopy settings—Section 3.1) and SEM-EDX (measuring trace (counter) elements) Section 3.3), additional MOCS samples from post filters of two other plants were used, as follows.

- MOCS from GWTP Onnen (Groningen, The Netherlands).

Table 2

Feed water quality, process design parameters and operational conditions of full scale GWTP De Punt and GWTP Grobendonk

Parameters feed water/technical information filter	Unit	De Punt	Grobendonk
Iron	mg/L	4.5–6.9	0.03–0.14
Manganese	mg/L	0.18–0.25	0.12–0.18
Ammonium	mg/L	0.29–0.78	<0.05–0.23
pH	[–]	7.3–7.5	7.5–7.6
Oxygen	mg/L	8–10	>10
Redox potential	mV	–50 to +50	+200 to +300
Type of aeration	–	spray	cascade
Position of filter	–	pre-filter	post-filter
Type of filtration	–	down flow	down flow
Type of filter media	–	quartz sand	anthracite/quartz sand
Grain size fraction virgin media	mm	1.8–2.4	0.8–1.8/0.4–0.8
Filter area	m <sup>2</sup>	12.5	37.5
Filter bed height	m	2	1.1 (0.6 + 0.5)
Flow per filter	m <sup>3</sup> /h	60	190
Filtration rate	m <sup>3</sup> /m <sup>2</sup> h	4.8	5.0
Empty bed contact time	min	25	13.2
Backwash (BW) criterion	–	head loss	head loss
Backwash frequency	n/week	2	0.5
Filter bed expansion during BW	–	no	yes (anthracite)
Filtered volume between BW	m <sup>3</sup> per filter run	5,000–7,000	10,000
Iron loading per filter run (FR)	kg Fe/m <sup>2</sup> FR	2.5	<0.1

The sample is taken from the top of the filter, in operation for more than 40 years.

- MOCS from GWTP Wierden (Vitens, The Netherlands).

The sample is taken from the top of the filter, in operation for more than 18 years.

### 2.1. Raman spectroscopy

With Raman spectroscopy it is possible to distinguish different (general) types of manganese oxides. For the Raman spectroscopy analysis a Horiba Jobin Yvon Labram instrument was used with the following settings (Table 3).

Exposure of the samples to high power laser radiation (5 mA) during Raman analysis for a long time (>120 s) may change the structure of the manganese oxides. However, under the applied conditions (Table 3), no structural damage was detected during the tests. Detailed information on the effect of high power radiation on structural changes of the manganese oxides is given in Section 3.1. Before analysis, the samples (either the integral grain or powder coating) were dried at room temperature to avoid excessive fluorescence caused by the presence of water in the samples.

Table 3

Parameter settings for Raman spectroscopy analysis

Parameter	Setting
Exposure	≥30 s
Current	0.05 mA
Confocal hole	1,000 μm
Slit	100 μm
Laser wave length	532.13 nm
Grating	600
Objective	x50
Density filter	D3
Detector	Synapse CCD
Detector size	1,024 pixels

### 2.2. XRD

XRD can be used to determine whether manganese oxide is crystalline or amorphous. Furthermore, this technique can provide additional information to clarify the sharpness of the peaks found with Raman spectroscopy. Most XRD measurements were carried out with a Bruker-D8 Advance diffractometer in Bragg-Brentano focusing geometry. The instrument was equipped with a Vantec PSD detector. Measurements were carried out at room temperature with the use of monochromatic

CoK $\alpha$ 1 radiation ( $\lambda = 0.179026$  nm). The  $2\theta$  scan was made in the range  $10$ – $110^\circ 2\theta$ , using a step size of  $0.038^\circ 2\theta$ . To check some of the analyses and to enhance their performance, some XRD measurements were also carried out with a Bruker-AXS D5005 diffractometer in Bragg-Brentano focusing geometry, equipped with a graphite monochromator in the diffracted beam. Before analysis, the samples were dried at room temperature and then pulverized to a size of  $10$ – $50$   $\mu\text{m}$ . The sample powder (for MOCS only the coating and for MOCA the coating including the anthracite grain) was put in an aluminium sample holder. The  $2\theta$  scan was made in the range  $10$ – $110^\circ 2\theta$ , using a step size of  $0.025^\circ 2\theta$  and a counting time of  $2$  s per step. The radiation was CuK $\alpha$ 1 ( $0.15406$  nm). Results obtained by both the XRD instruments were evaluated with the internal Bruker EVA software.

### 2.3. SEM-EDX

SEM pictures show the structure of the coating and the manganese oxide inside. In addition, EDX provides information about the trace (counter) elements present in these structures. Therefore, differences in peak ratio found with Raman spectroscopy can be clarified. The SEM pictures were made with a JEOL-6480LV. Samples (either the integral grain or powder coating) were placed on  $15$  mm diameter mounts with a double-sided carbon adhesive tab. The SEM was operated both under High Vacuum (HV) and Low Vacuum (LV) conditions.

Before observation under HV conditions, the samples were coated in a JEOL JFC-1200 fine coater with a thin ( $10$  nm) Au layer. The operation under HV conditions was done at  $6$  kV at  $10$  mm Working Distance (WD) and Spot Size (SS)  $20$ . Samples were also investigated without Au coating under LV conditions at  $10$  kV and SS  $60$ . Composition of the adsorbed coating layers was determined with an X-ray microanalysis (EDX) System type Noran System SIX from the Thermo Electron Corporation. Analyses were done at  $10$  kV and SS  $70$  for both the Au-coated samples at HV conditions and non-coated samples at LV conditions. In the latter, no Au peaks were observed in the EDX spectrum.

### 2.4. EPR

Once the MnO $_x$  is characterized as “a type of Birnessite”, EPR can be employed to identify the exact type of Birnessite and additionally also to determine the origin of the Birnessite. For EPR the whole grain was always used.

EPR analyses were carried out with a Bruker instrument operating at  $9.46$  GHz (W-waveband). The analyses were carried out at two different temperatures, i.e. at  $77$  K (cooled with nitrogen) and  $298$  K (room temperature).

## 3. Results and discussion

### 3.1. Raman spectroscopy

#### 3.1.1. Selection Raman spectroscopy settings

As explained in Section 2.1, the structure of almost all manganese (oxide) compounds (except Hausmannite) is subjected to Raman spectroscopic changes when exposed to a high current [24,25]. Laser irradiation in excess of  $5$  mA for longer than  $120$  s causes structural changes of the exposed compounds (polymorphism). To prevent these changes, the current of the laser in this study was limited to  $0.05$  mA. The differences in spectra obtained with high ( $5$  mA,  $>120$  s) and low ( $0.05$  mA) radiation intensities are shown in Fig. 3.

From the two spectra in Fig. 3 it can be seen that high intensity laser irradiation changes the position of the peaks, as well as the pattern of the spectrum. According to [24,25], high current irradiation transforms all MnO $_x$  samples (and therefore also Birnessite) into Mn $_3$ O $_4$  (Hausmannite). Hausmannite is very stable when exposed to a Raman laser, so its structure is not changed by the high level of irradiation. Furthermore, due to its crystalline lattice structure it displays a sharp peak in the Raman spectrum. To ascertain this transformation, Raman profiles of Birnessite from this study and an MnO $_2$  reference sample (Alfa Aesar) were exposed to high current radiation ( $5$  mA,  $>120$  s), and compared to a Hausmannite spectrum from the RRUFF database [26] (Fig. 4).

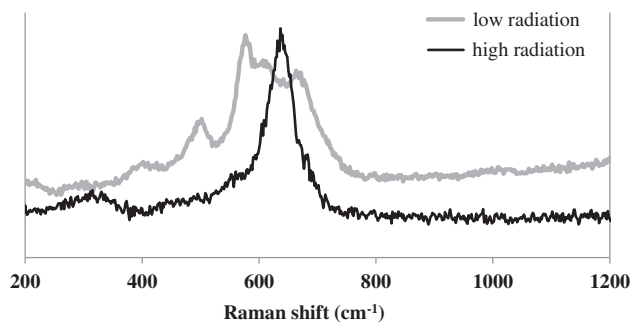


Fig. 3. Raman spectra at  $532$  nm of MOCS (Onnen), exposed to low (grey line) and high laser radiation (black line).

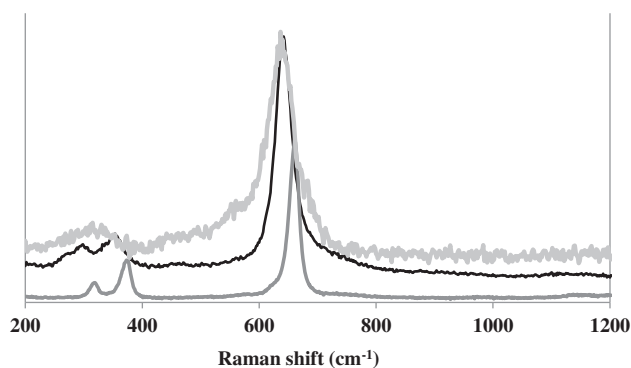


Fig. 4. Raman spectra (at 532 nm) of Birnessite from a sample of this study (light grey line) and  $\text{MnO}_2$  reference (black line) after exposure to 5 mA for >120 s, compared to a Hausmannite spectrum (dark grey line) from the RRUFF database [26].

From Fig. 4, it can be seen that the spectra of Birnessite in a sample from this study as well as the  $\text{MnO}_2$  reference, exposed to high laser radiation, show a close resemblance to the spectrum of Hausmannite. This indicates that both manganese oxides (Birnessite and  $\text{MnO}_2$ ) underwent structural changes when exposed to high laser power, as stated by [25].

### 3.1.2. Characterization of MOCA and MOCS by Raman spectroscopy

The Raman spectra of manganese-coated samples from four GWTPs are presented in Fig. 5. From Fig. 5, it can be seen that the spectral patterns of all samples were similar, indicating a similar type of manganese oxide. The three most pronounced absorbance peaks were found at Raman shifts of 495–505, 570–575 and 635–655  $\text{cm}^{-1}$ , typical for the Birnessite group of manganese oxides [24]. All spectra exhibited a less pronounced peak at a Raman shift at 400–420  $\text{cm}^{-1}$ . The undulating peaks were typical for oxides with a poorly crystalline structure, such as Birnessite [27].

To confirm the presence of Birnessite, the spectra of the MOCS/MOCA samples were compared with the spectra of synthetically produced Birnessite [28], shown in Fig. 6(A). Comparison of the spectra produced in this study with previously reported results strongly suggested that the manganese oxide in the coating of the MOCS and MOCA samples was of a Birnessite type.

The spectra of MOCS and MOCA samples were also compared with a Raman profile of a reference sample of naturally formed Birnessite (Fig. 6(B)), obtained from the Aufgeklärt Glück mine in

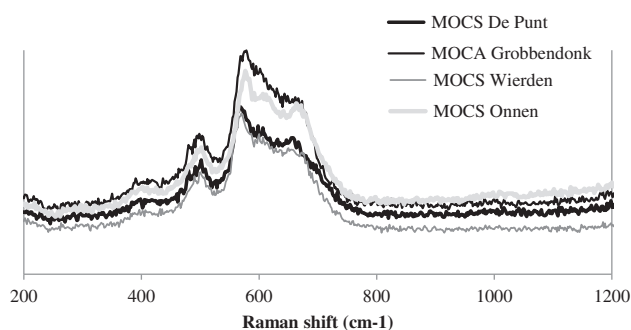


Fig. 5. Raman spectra (at 532 nm) of the four MOCS/MOCA samples.

Hasserode, the Harz Mountains, Sachsen-Anhalt, Germany [29].

Fig. 6(B) shows that the main peaks from the Birnessite reference as well as the MOCA and MOCS samples were on the same Raman shift. Only the ratio and height of the peaks varied between the different samples and the reference, probably due to a different concentration of counter ions in the materials [24,25], as shown by SEM-EDX (Section 3.3, Table 4).

The Raman spectra strongly suggested that the manganese oxides in the MOCA and MOCS samples were of a Birnessite type.

In order to exclude the presence of other manganese oxides in the coatings, the Raman spectra of samples from this study were compared with the reference spectra of four other manganese oxides Pyrochroite (A), Hausmannite (B), Manganite (C) and Pyrolusite (D) (Fig. 7). Spectra A–C were taken from the RRUFF database [26] and spectrum D from the measured reference sample (Alfa Aesar).

The four manganese oxides displayed one peak in the same region as the MOCS/MOCA samples between 630 and 650  $\text{cm}^{-1}$ . This wavelength is characteristic for all manganese oxides and not indicative of a particular one. Therefore, it was concluded that apart from Birnessite no other manganese oxides were present in the coating of the filter media.

### 3.2. XRD

Fig. 8 shows an XRD spectrum of MOCS coating from GWTP De Punt (black line) and a MOCA coating from GWTP Grobbendonk (grey line). The analysed MOCA sample contained some crushed anthracite (carbon) since it was impossible to separate the coating completely from the anthracite.

From Fig. 8 it can be seen, as already shown by the Raman spectroscopy that the MOCS coating was poorly crystalline. The only peak ( $31^\circ$ ,  $2\theta$ ) belonged to

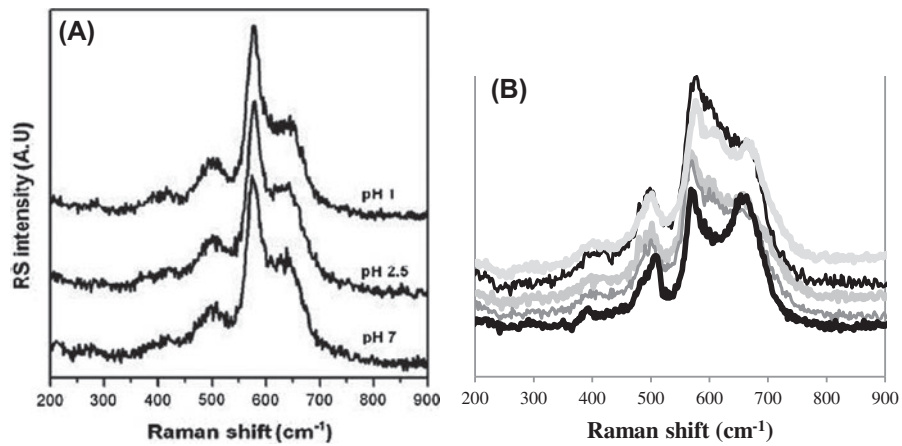


Fig. 6. (A) Raman spectra of synthetically produced Birnessite at 514 nm [28]. (B) Raman spectra of samples from this study (grey lines) compared to the spectrum of the Birnessite reference (bold black line).

Table 4  
SEM-EDX analysis of counter (trace) elements in weight (%)

	MOCA Grobbendonk	MOCS De Punt	MOCS Onnen	MOCS Wierden
Aluminium (Al)	0.5	<0.1	0.6	<0.1
Calcium (Ca)	6.8	2.3	7.2	7.7
Magnesium (Mg)	0.3	<0.1	0.4	0.3
Potassium (K)	0.2	<0.1	<0.1	<0.1
Silica (Si)	1.0	5.9	2.6	0.9
Sodium (Na)	<0.1	<0.1	0.2	<0.1

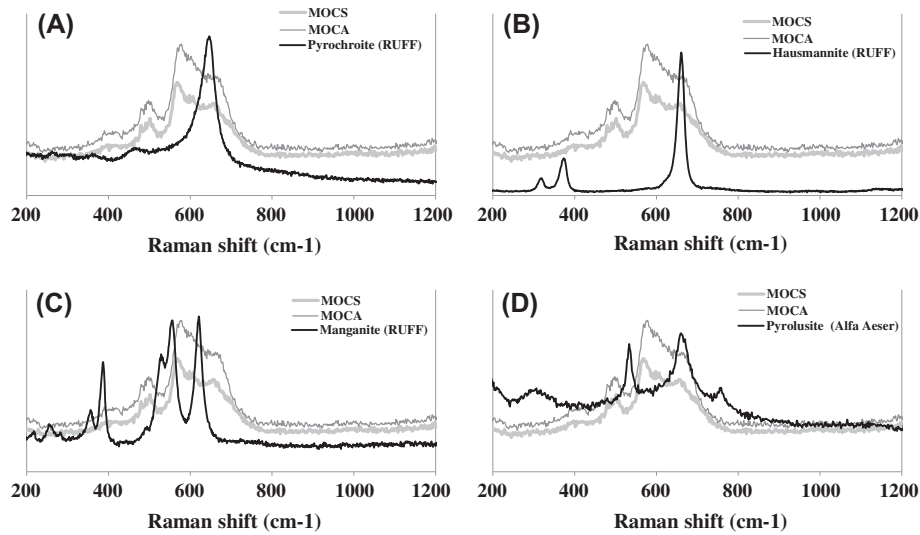


Fig. 7. Raman spectra at low power and 532 nm of MOCS De Punt and MOCA Grobbendonk, compared to (A) Pyrochroite, (B) Hausmannite, (C) Manganite and (D) Pyrolusite.

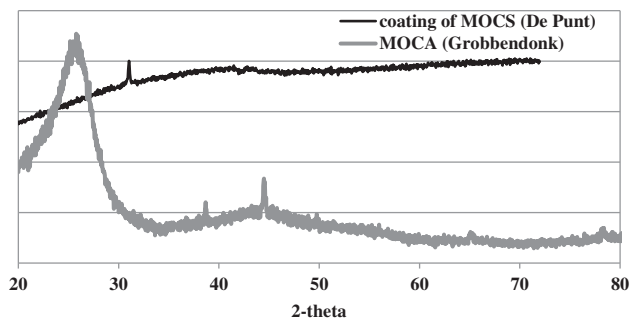


Fig. 8. XRD spectra (conducted with a Bruker D8), of pulverized MOCS coating and MOCA (the latter including crushed anthracite core).

silica originating from the filter media. Additional (sharp) peaks were not present in the spectra from the MOCS sample, so no crystalline  $\text{MnO}_x$  was present on the MOCS. Also, no crystalline  $\text{MnO}_x$  was found on the MOCA. The few small peaks and the broad peak in the MOCA sample ( $25^\circ$ ,  $2\theta$ ) originate from carbon or graphite (C) from crushed anthracite, that could not be removed completely from the coating (as mentioned above).

For comparison, the XRD spectra of three Alfa Aesar reference manganese oxides i.e.  $\text{MnO}$ ,  $\text{Mn}_2\text{O}_3$  and  $\text{MnO}_2$  with crystalline structure are presented in Fig. 9.

Contrary to the MOCA and MOCS coating, the XRD spectra of the three reference manganese oxides showed sharp peaks and the  $2\theta$  positions of the peaks were confirmed by the reference XRD spectra of oxides from the internal Bruker EVA database. If the manganese oxide in the samples from this study had been crystalline, sharp peaks should have been observed similar to the spectra of the three reference manganese oxides. The absence of sharp peaks confirmed the amorphous character of the sample coating. Thus, the XRD results also confirmed that the

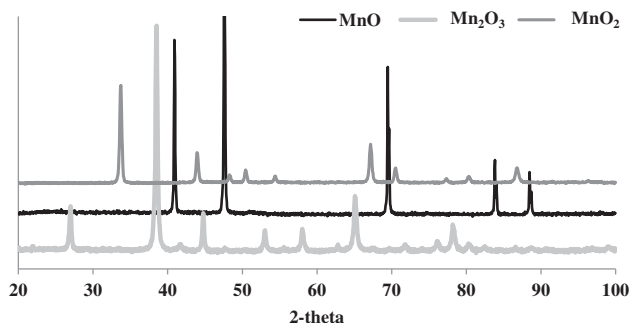


Fig. 9. XRD spectra of reference manganese oxides:  $\text{MnO}$ ,  $\text{Mn}_2\text{O}_3$  and  $\text{MnO}_2$  (Alfa Aesar).

manganese oxide(s) in the MOCS and MOCA samples were not crystalline manganese oxides (i.e.  $\text{MnO}_2$ ,  $\text{Mn}_2\text{O}_3$  or  $\text{MnO}$ ).

### 3.3. SEM-EDX

In Fig. 10a SEM image of virgin quartz (sand) filter media is shown. Fig. 10 shows that the surface of virgin sand was not completely smooth, indicating a high porosity and specific surface area, and therefore probably contained many sites for attachment of bacteria and/or manganese, which could shorten the ripening time.

In Fig. 11 SEM images of MOCS and MOCA samples are shown.

Images A and B in Fig. 11 confirm the Raman spectroscopy results and the XRD analysis that the manganese coating was poorly crystalline.

Results of the SEM-EDX analyses show that apart from manganese and iron, the coating of the filter media contained (trace) elements such as aluminium, calcium, magnesium, potassium, sodium and/or silica (Table 4).

The counter (trace) elements in Table 4 are of importance with respect to the ratio and height of the Raman peaks, as discussed in Section 3.1 and shown in Fig. 6(B). Counter ions present in filter media coatings may also impact the adsorptive properties of the coating.

### 3.4. EPR

In Fig. 12 the EPR spectra of MOCS De Punt measured at two temperatures (298 K—room temperature

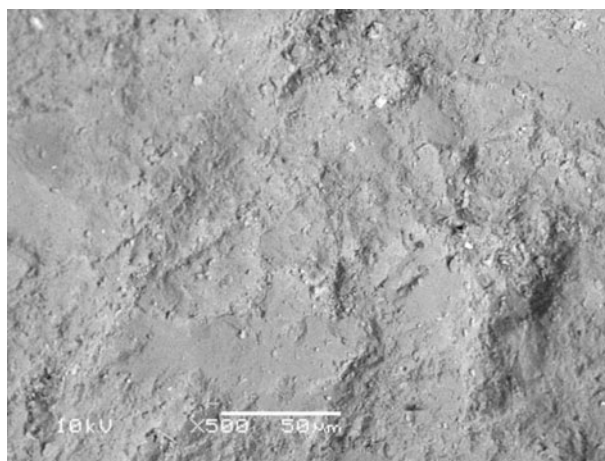


Fig. 10. SEM image of virgin quartz media (sand); 500 $\times$  magnification.

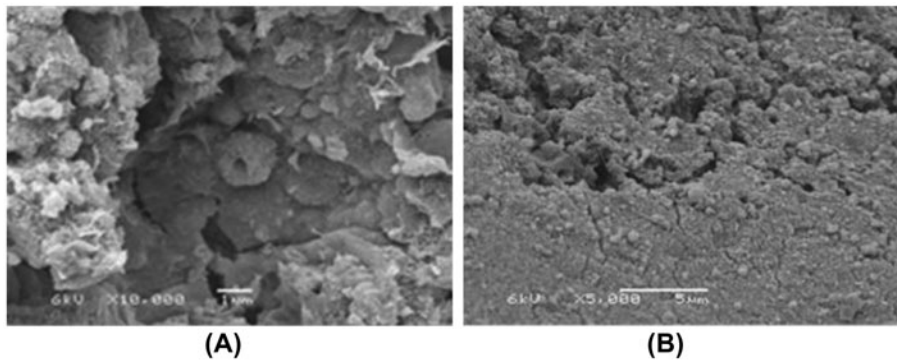


Fig. 11. SEM images of filter media coating. (A) MOCS De Punt; 10,000×. (B) MOCA Grobbendonk; 5,000×.

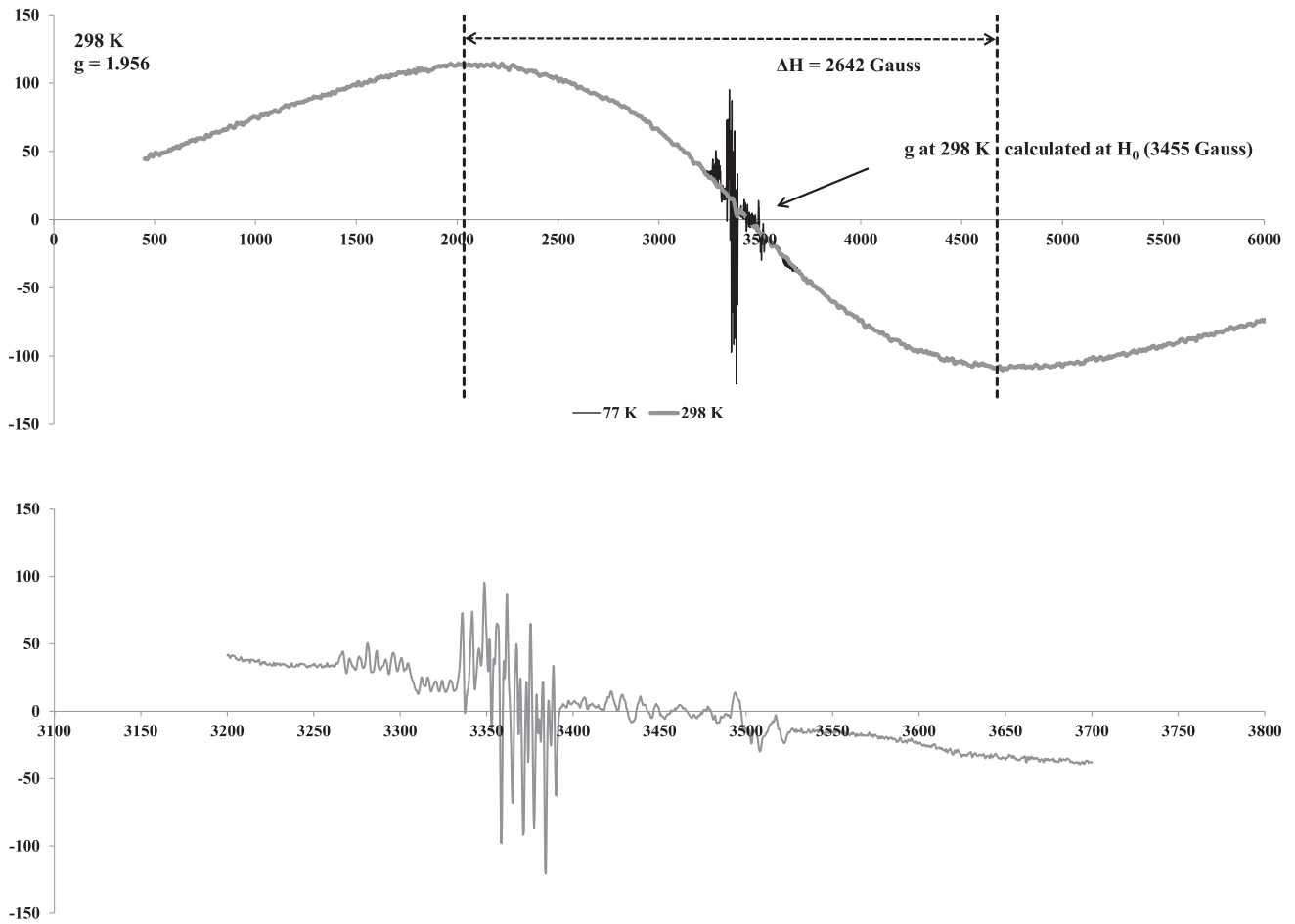


Fig. 12. EPR spectra of MOCS De Punt.

Notes: Top half: spectra measured at 298 K (grey line) and 77 K (black line). Bottom half: expanded spectrum measured at 77 K.

and 77 K) are shown. Due to the analytical interference of carbon (originating from anthracite), it was not

possible to obtain a complete EPR spectrum for MOCA Grobbendonk.

The detailed EPR pattern (Fig. 12, the bottom half) shows the “6 line hyperfine structure of manganese”. This pattern is typical for oxides containing manganese ions with a different valence, including  $\text{Mn}^{2+}$  [30]. Birnessite has a valence between 3.5 and 3.9 [18,27,31], due to the presence of  $\text{Mn}^{3+}$  and  $\text{Mn}^{4+}$  in the lattice. This pattern is an additional indication that the predominant manganese component of the MOCS coating is a manganese oxide, containing manganese ions with different oxidation numbers, such as Birnessite.

Generally, EPR spectra are characterized by two parameters: (i) the line width:  $\Delta H$  in gauss and (ii) the spectroscopic splitting factor:  $g$  (g-factor). EPR was used to investigate the origin of different types of Birnessite [31]. These values of  $\Delta H$  measured at 77 and 298 K and the  $g$ -factor calculated at 298 K are characteristic of Birnessite.

$\Delta H$  is measured as the distance between the highest and lowest point of the signal wave, and the  $g$  factor is calculated from the spectrometer microwave frequency ( $y$ ) and the magnetic field ( $H_0$ ) applied during the analysis when the signal is zero (Eq. 1):

$$g = \frac{h}{\mu_B} \times \frac{y}{H_0} \quad (1)$$

where

$h$  = Planck constant ( $6.62 \times 10^{-34}$  Js);

$\mu_B$  = Bohr magneton ( $9.27 \times 10^{-28}$  J/G);

$y$  = spectrometer microwave frequency (GHz);

$H_0$  = applied magnetic field where signal is zero (gauss).

$\Delta H$  values measured at 298 and at 77 K were 2,642 gauss and 3,950 gauss, respectively (Fig. 12—top half). Taking into account the applied magnetic field ( $H_0$ ) of 3,455 gauss at 298 K, the calculated  $g$  factor was 1.956. Comparing the EPR results from this study with the data reported by [31], a few conclusions can be drawn. Firstly, the EPR analysis confirmed the results obtained by Raman spectroscopy that the manganese oxide on MOCS is Birnessite. Next, comparing the two  $\Delta H$  values and the  $g$  factor with the results from [31] shows that the Birnessite in the coating of MOCS De Punt was of physicochemical origin. However, this does not mean that the growth of manganese oxide on the virgin filter media (ripening process) starts exclusively chemically. The MOCS sample from GWTP De Punt was taken after more than 15 years of operation, and consequently the EPR analysis only confirmed the physicochemical nature of Birnessite after this elapsed time.

### 3.5. The importance of Birnessite formation on MOCA/MOCS for manganese removal

The mineral Birnessite was found in 1956 in a small hamlet called Birness, Scotland, UK [32]. At that time it was a new mineral to which the name Birnessite, after the locality, was given. Its molecular structure was given as  $(\text{Na}_{0.7}\text{Ca}_{0.3})\text{Mn}_7\text{O}_{14} \cdot 2.8\text{H}_2\text{O}$ . In time, different formulas were proposed for Birnessite, indicating there is no single structure, but different compositions exist (“minerals of the Birnessite type”). From this study, it can be observed that Birnessite was the manganese compound formed during filter ripening, and predominantly present in all manganese oxide coatings extracted from the four GWTPs that showed complete manganese removal. Consequently, Birnessite appears to be of particular importance for manganese removal in conventional aeration-filtration groundwater treatment plants. The presence of Birnessite may provide an explanation for the very effective manganese removal in these filters in practice. Birnessite is extremely suitable to remove manganese, because of its structure as described by Post [27]: “the Birnessite group of minerals has layered structures, which may readily undergo oxidation-reduction and cation-exchange reactions and play a major role in controlling groundwater chemistry”. The high cation exchange and adsorption capacity of Birnessite is also described by several other researchers [10,33–39]. Thus, Birnessite is very suitable to adsorb  $\text{Mn}^{2+}$ .

The Birnessite group of minerals (including Buserite) is also important, because of its high reactivity [27,40]. In Buserite and Birnessite the average valence number of manganese ranges from +3.5 to +3.9 [18]. Although restricted compared to other manganese oxides, further oxidation of Buserite and Birnessite is still possible. The combination of properties makes Birnessite a highly reactive manganese oxide, with very good adsorptive properties for dissolved manganese, and its subsequent autocatalytic oxidation. The knowledge that Birnessite is the manganese oxide responsible for efficient manganese removal can help substantially accelerate the ripening process of virgin filter media, by creating conditions favouring the formation of Birnessite. Knowing that the oxidation from  $\text{Mn}^{2+}$  into Pyrolusite [16], via Birnessite (Pyrochroite  $\rightarrow$  Buserite/Birnessite  $\rightarrow$  Nsutite  $\rightarrow$  Pyrolusite, Fig. 2), is only possible under (very) alkaline conditions [41], it is not likely that a fast filter ripening of virgin filter media starts in a chemical way, without oxidant dosage. Therefore, the formation of the manganese coating may be initiated by bacterial activity.

Several researchers have suggested that manganese removal is influenced by bacteria (e.g. *Pseudomonas* sp., *Leptothrix* sp.), which are able to oxidize  $Mn^{2+}$  [31,42–52]. Therefore, the ripening of the filter media probably starts with the biological formation of Birnessite. In time very fast physicochemical auto-catalytic adsorption/oxidation reactions may become more important and result in production of Birnessite of physicochemical origin, whose presence is shown in this study. However, further research is required to support this hypothesis.

#### 4. Conclusions

The Raman spectroscopy, XRD and SEM analyses carried out in this study showed that the manganese oxide in the coating of the manganese removing filter media is poorly crystalline. Raman spectroscopy and EPR analysis further clarified that the predominant manganese oxide, responsible for effective removal of dissolved manganese, is of a Birnessite type. Calculation of  $\Delta H$  and the  $g$  factor from EPR analysis and comparison of these parameters with results from literature identified Birnessite as being of physicochemical origin, but the sampling after a ripening period of about 15 years does not exclude the possibility of Birnessite formation starting via a biological pathway. Despite the generally accepted theory that the manganese oxidation pathway is via Hausmannite and Manganite, the results transpiring from this research imply that in water treatment practice oxidation of manganese on the surface of manganese removal filter media is more likely to form a Birnessite type of manganese oxide. Birnessite has very good properties for adsorption and autocatalytic oxidation of dissolved manganese. Identification of Birnessite as the predominant manganese oxide in filter media that effectively remove manganese could possibly enable shortening ripening time in conventional aeration-filtration groundwater treatment plants by creating conditions that favour the formation of this compound.

#### Acknowledgements

This research is financially and technically supported by WLN and by the Dutch water companies Waterbedrijf Groningen (WBG) and Waterleiding Maatschappij Drenthe (WMD). The authors of this paper would like to thank Mr Arie Zwijnenburg and Mr Ton van der Zande from Wetsus, Centre of Excellence for Sustainable Water Technology, Mr Wesley Browne from the University of Groningen and Mr Ruud Hendrikx of the Department of Materials

Science and Engineering from the Technical University of Delft for their help with the analyses of samples and interpretation of the results. The authors would also like to thank the Belgian water company Pidpa and the Dutch water company Vitens for providing filter media for this study and their willingness to disclose their groundwater treatment plant data. Finally, we would like to thank Dr Thomas Witzke (mineralogist) for donating a naturally formed Birnessite reference sample.

#### References

- [1] UNEP, Vital water graphics. (2008). Available from: <http://www.unep.org/dewa/vitalwater/index.html>.
- [2] B. Cools, Vlaamse Maatschappij voor Watervoorziening [Flemish water company] (VMW), personal communication, Belgium, 2010.
- [3] K. Huysman, Provinciale en Intercommunale Drinkwatermaatschappij der Provincie Antwerpen [Pidpa: department of process technology and water quality] (PIDPA), personal communication, Belgium, 2010.
- [4] J. Krull, Stadtwerke Emden [water company Emden] (SWE), personal communication, Germany, 2010.
- [5] R. Buamah, B. Petrusevski, J.C. Schippers, Adsorptive removal of manganese(II) from the aqueous phase using iron oxide coated sand, *J. Water Supply Res.* 57 (1) (2008) 1–11.
- [6] R. Buamah, Adsorptive removal of manganese, arsenic and iron from groundwater, PhD thesis, UNESCO-IHE Delft/Wageningen University, The Netherlands, 2009.
- [7] R. Buamah, B. Petrusevski, D. de Ridder, S. van de Watering, J.C. Schippers, Manganese removal in groundwater treatment: practice, problems and probable solutions, *Water Sci. Technol.* 9(1) (2009) 89–98.
- [8] P.Y. Hu, Y.H. Hsieh, J.C. Chen, C.Y. Chang, Adsorption of divalent manganese ion on manganese-coated sand, *J. Water Supply Res.* T. 53(3) (2004) 151–158.
- [9] A.A. Islam, J.E. Goodwill, R. Bouchard, J.E. Tobiasen, W.R. Knocke, Characterization of filter media  $MnO_2(s)$  surfaces and Mn removal capability, *J. Am. Water Works Assoc.* 102(9) (2010) 71–83.
- [10] W.G. Kim, S.J. Kim, S.M. Lee, D. Tiwari, Removal characteristics of manganese-coated solid samples for Mn(II), *Desal. Wat. Treat.* 4 (2009) 218–223.
- [11] K. Olanczuk-Neyman, R. Bray, The role of physicochemical and biological processes in manganese and ammonia nitrogen removal from groundwater, *Pol. J. Environ. Stud.* 9(2) (2000) 91–96.
- [12] D.M. Sahabi, M. Takeda, I. Suzuki, J.I. Koizumi, Removal of  $Mn^{2+}$  from water by ‘aged’ biofilter media: The role of catalytic oxides layers, *J. Bio. Sci. Bioeng* 107(2) (2009) 151–157.
- [13] T. Stembal, M. Markic, N. Ribicic, F. Briski, L. Sipos, Removal of ammonia, iron and manganese from groundwaters of northern Croatia—Pilot plant studies, *Process Biochem.* 40 (2005) 327–335.
- [14] A.G. Tekerlekopoulou, D.V. Vayenas, Simultaneous biological removal of ammonia, iron and manganese from potable water using a trickling filter, *Biochem. Eng. J.* 39 (2008) 215–220.

- [15] D. Tiwari, M.R. Yu, M.N. Kim, S.M. Lee, O.H. Kwon, K.M. Choi, G.J. Lim, J.K. Yang, Potential application of manganese coated sand in the removal of Mn(II) from aqueous solutions, *Water Sci. Technol.* 56(7) (2007) 153–160.
- [16] W. Stumm, J.J. Morgan, *Aquatic Chemistry, Chemical Equilibria and Rates*. 3rd ed. Wiley, New York, NY, 1996, pp. 464–467.
- [17] P. Anschutz, K. Dedieu, F. Desmzes, G. Chaillou, Speciation, oxidation state, and reactivity of particulate manganese in marine sediments, *Chem. Geol.* 218 (2005) 265–279.
- [18] H. Cui, G. Qiu, X. Feng, W. Tan, F. Liu, Birnessites with different average manganese oxidation states synthesized, characterized, and transformed to todorokite at atmospheric pressure, *Clay. Clay Miner.* 57 (6) (2009) 715–724.
- [19] K.H. Carlson, W.R. Knocke, K.R. Gertig, Optimizing treatment through Fe and Mn fractionation, *J. Am. Water Works Assoc.* 89(4) (1997) 162–171.
- [20] W.R. Knocke, J.E. van Benschoten, M.J. Kearney, A.W. Soborski, D.A. Reckhow, Kinetics of manganese and iron oxidation by Potassium Permanganate and chlorine dioxide, *J. Am. Water Works Assoc.* 83(6) (1991) 80–87.
- [21] A. Graveland, Removal of manganese from groundwater, PhD thesis, Technical University Delft, The Netherlands, 1971.
- [22] A. Graveland, P.M. Heertjes, Removal of manganese from groundwater by heterogeneous autocatalytic oxidation, *Trans. Inst. Chem. Eng.* 53 (1975) 154–164.
- [23] P.Y. Hu, Y.H. Hsieh, J.C. Chen, C.Y. Chang, Characteristics of manganese-coated sand using SEM and EDAX analysis, *J. Colloid Interf. Sci.* 272 (2004) 308–313.
- [24] C. Julien, M. Massot, R. Baddour-Hadjean, S. Franger, S. Bach, J.P. Pereira-Ramos, Raman spectra of Birnessite manganese dioxides, *Solid State Ionics* 159 (2003) 345–356.
- [25] C. Julien, M. Massot, C. Poinسیون, Lattice vibrations of manganese oxides, *Spectrochim. Acta A* 60 (2004) 689–700.
- [26] R.T. Downs, The RRUFF Project: An integrated study of the chemistry, crystallography, Raman and infrared spectroscopy of minerals. Program and abstracts of the 19th general meeting of the international mineralogical association in Kobe, Japan, 2006.
- [27] J.E. Post, Manganese oxide minerals: Crystal structures and economic and environmental significance, *Proc. Nat. Acad. Sci. U.S.A.* 96 (1999) 3447–3454.
- [28] S.B. Ma, K.Y. Ahn, E.S. Lee, K.W. Oh, K.B. Kim, Synthesis and characterization of manganese dioxide spontaneously coated on carbon nanotubes, *Carbon* 45 (2007) 375–382.
- [29] T. Witzke, mineralogist, PANanalytical, personal communication, Germany, 2012.
- [30] W.R. Browne, Assistant professor, Stratingh Institute for Chemistry, University of Groningen, personal communication, The Netherlands, 2011.
- [31] S.S. Kim, J.R. Bargar, K.H. Nealson, B.E. Flood, J.L. Kirschvink, T.D. Raub, B.M. Tebo, M. Villalobos, Searching for biosignatures using electron paramagnetic resonance (EPR) analysis of manganese oxides, *Astrobiology* 11(8) (2011) 775–786.
- [32] L.H.P. Jones, A.A. Milne, Birnessite, a new manganese oxide mineral from Aberdeenshire, Scotland, *Mineral. Mag.* 31(235) (1956) 283–288.
- [33] D.C. Golden, J.B. Dixon, C.C. Chen, Ion exchange, thermal transformations, and oxidizing properties of Birnessite, *Clays Clay Miner.* 34(5) (1986) 511–520.
- [34] R. Han, W. Zou, Z. Zhang, J. Shi, J. Yang, Removal of copper(II) and lead(II) from aqueous solution by manganese oxide coated sand, *J. Hazard. Mater.* 137 (2006) 384–395.
- [35] I. Kim, S. Jung, Soluble manganese removal by porous media filtration, *Environ. Technol.* 29 (2008) 1265–1273.
- [36] S.M. Lee, D. Tiwari, K.M. Choi, Jae-Kyu Yang, Yoon-Young Chang, H.D. Lee, Removal of Mn(II) from Aqueous Solutions Using Manganese-Coated Sand Samples, *J. Chem. Eng. Data.* 54 (2009) 1823–1828.
- [37] J. Murray, The interaction of metal ions at the manganese dioxide-solution interface, *Geochim. Cosmochim. Ac.* 39 (1976) 606–619.
- [38] P.J. Pretorius, P.W. Linder, The adsorption characteristics of  $\delta$ -Manganese dioxide: A collection of diffuse double layer constants for the adsorption of  $H^+$ ,  $Cu^{2+}$ ,  $Ni^{2+}$ ,  $Zn^{2+}$ ,  $Cd^{2+}$  and  $Pb^{2+}$ , *Appl. Geochem.* 16 (2001) 1067–1082.
- [39] D.A. White, A. Asfar-Siddique, Removal of Manganese and iron from drinking water using hydrous Manganese Dioxide, *Solvent Extr. Ion Exch.* 15(6) (1997) 1133–1145.
- [40] J.E. Post, D.R. Veblen, Crystal structure determinations of synthetic sodium, magnesium, and potassium Birnessite using TEM and the Rietveld method, *Am. Mineral.* 7(5) (1999) 477–489.
- [41] X. Feng, W. Tan, F. Liu, Q. Huang, X. Liu, Pathways of Birnessite formation in alkali medium, *Sci. China Ser D.* 48(9) (2005) 1438–1451.
- [42] J.R. Barger, B.M. Tebo, U. Bergmann, S.M. Webb, P. Glatzel, V.Q. Chiu, M. Villalobos, Biotic and abiotic products of Mn(II) oxidation by spores of the marine *Bacillus* sp. strain SG-1, *Am. Mineral.* 90 (2005) 143–154.
- [43] M.S. Burger, S.S. Mercer, G.D. Shupe, G.A. Gagnon, Manganese removal during bench-scale biofiltration, *Water Res.* 42 (2008) 4733–4742.
- [44] M.S. Burger, C.A. Krentz, S.S. Mercer, G.A. Gagnon, Manganese removal and occurrence of manganese oxidizing bacteria in full-scale biofilters, *J. Water Supply Res. T.* 57(5) (2008) 351–359.
- [45] K. Geszvain, Mn(II) oxidation in *Pseudomonas putida* GB-1 is influenced by flagella synthesis and surface substrate, *Arch. Microbiol.* 193 (2011) 605–614.
- [46] I.A. Katsoyiannis, A.I. Zouboulis, Biological treatment of Mn(II) and Fe(II) containing groundwater: Kinetic considerations and product characterization, *Water Res.* 38 (2004) 1922–1932.
- [47] B.M. Tebo, J.R. Marger, B.G. Clement, G.J. Dick, K.J. Murray, D. Parker, R. Verity, S.M. Webb, Biogenic Manganese oxides: Properties and mechanisms of formation, *Annu. Rev. Earth Pl. Sci.* 32 (2004) 287–328.
- [48] M. Villalobos, B. Toner, J. Barger, G. Sposito, Characterization of the manganese oxide produced by *Pseudomonas putida* strain MnB1, *Geochim. Cosmochim. Ac.* 67(14) (2003) 2649–2662.

- [49] J. Vandenabeele, D. de Beer, R. Germonpré, W. Verstrete, Manganese oxidation by microbial consortia from sand filters, *Microb. Ecol.* 24 (1992) 91–108.
- [50] J. Vandenabeele, M. van de Woestyne, F. Houwen, R. Germonpré, D. Vandesaende and W. Verstrete, Role of autotrophic nitrifiers in biological manganese removal from groundwater containing manganese and ammonium, *Microb. Ecol.* 28 (1995) 83–98.
- [51] J. Vandenabeele, Manganese removal by microbial consortia from rapid sand filters treating water containing  $Mn^{2+}$  and  $NH_4^+$ , PhD thesis, Gent, Belgium, 1993.
- [52] A.G. Tekerlekopoulou, I.A. Vasiliadou, D.V. Vayenas, Biological manganese removal from potable water using trickling filters, *Biochem. Eng. J.* 38 (2008) 292–301.